

THE
UNIVERSITY
OF RHODE ISLAND

University of Rhode Island
DigitalCommons@URI

Natural Resources Science Faculty Publications

Natural Resources Science

2-15-2018

Identification of a putative man-made object from an underwater crash site using CAD model superimposition

Jay Vincelli

Fatih Calakli

Michael Stone

Graham E. Forrester

Timothy Mellon

See next page for additional authors

Follow this and additional works at: https://digitalcommons.uri.edu/nrs_facpubs

**The University of Rhode Island Faculty have made this article openly available.
Please let us know how Open Access to this research benefits you.**

This is a pre-publication author manuscript of the final, published article.

Terms of Use

This article is made available under the terms and conditions applicable towards Open Access Policy Articles, as set forth in our [Terms of Use](#).

Authors

Jay Vincelli, Fatih Calakli, Michael Stone, Graham E. Forrester, Timothy Mellon, and John Jarrell

1 **Identification of a putative man-made object from an underwater crash site using CAD model**
2 **superimposition**

3 A comparison of unique features on an underwater object are compared to the features of a known object
4 modeled in CAD to assess its likelihood as being a component from a downed plane at the suspected
5 incident scene.

6 Jay M. Vincelli^a, jvincelli@materialsscience.org

7 Fatih Calakli^{a,b}, fatih_calakli@brown.edu

8 Michael Stone^{a,c}, sstone@materialsscience.org

9 Graham E. Forrester^c, gforrester@uri.edu

10 Timothy D. Mellon, panam.captain@yahoo.com

11 John D. Jarrell^{a,b}, johnjarrell@materialsscience.org

12

13 ^a Materials Science Associates, 315 Commerce Park Rd, Unit 1, North Kingstown, RI 02893

14 ^b Brown University, 182 Hope St, Providence, RI 02912

15 ^c University of Rhode Island, Dept. of Natural Resources Science, Kingston, RI 02881

16

17 **Keywords:** Vehicle accident; video analysis; Amelia Earhart; aircraft

18

19 **Abstract**

20 In order to identify an object in video, a comparison with an exemplar object is typically needed.

21 In this paper, we discuss the methodology used to identify an object detected in underwater video that was

22 recorded during an investigation into Amelia Earhart's purported crash site. A computer aided design

23 (CAD) model of the suspected aircraft component was created based on measurements made from

24 orthogonally rectified images of a reference aircraft, and validated against historical photographs of the

25 subject aircraft prior to the crash. The CAD model was then superimposed on the underwater video, and

26 specific features on the object were geometrically compared between the CAD model and the video. This

- 27 geometrical comparison was used to assess the goodness of fit between the purported object and the
- 28 object identified in the underwater video.

29 1. Introduction

30 Finding and identifying pieces of manmade wreckage in underwater environments can be
31 challenging. Many types of information must be taken into consideration when identifying objects, such
32 as texture, pattern, and color differences. The size and dimensions of objects are also critical and, unless
33 the object is retrieved, must be derived from scaling information plus relative and absolute position. There
34 are many different methods to survey and document artifacts with a wide range of ease and accuracy. [1].
35 Cost and availability are major determining factors when choosing the best way to carry out a survey.
36 Depending on the depth and location, methods can range from side scan sonar to having a diver on site to
37 perform running distance based measurements (Barkai and Kahanov 2007; Telem and Filin 2013).
38 Affordable precise digital cameras are widening the relevancy of photogrammetry in many disciplines.
39 Image based analysis can significantly cut down the man hours needed to identify objects compared to
40 traditional hands-on approaches [4]. Many image based reconstruction methods, based on
41 photogrammetry and geometric principles are available. Stereo cameras can be very effective but require
42 precise calibration and complexity that is too costly for many applications [5]. Approaches for monocular
43 cameras include structure from motion (SfM) [6], projection of structured light [7], and depth from
44 defocus [8]. These methods often require high quality recording and very structured illumination. [9].
45 Underwater photogrammetry provides an efficient and nondestructive mechanism for sampling
46 environments with limited accessibility. In the absence of enough information to create a dense
47 reconstruction of an object, geometric comparisons can be sufficient to identify objects.

48 In this retrospective analysis, we were provided with video footage from which we were tasked with
49 identifying any pieces of wreckage and verifying their connection to a wrecked aircraft. The video was
50 taken with a monocular camera on a remote controlled underwater vehicle (ROV). The site was located
51 on a Pacific atoll at 200-300 m depth and so, because of its remoteness, there was no opportunity to return
52 at a later date to take better or closer video of objects identified after filming. As a result, a different, off-
53 site approach for identification of objects in the video was needed. Man-made objects would likely be
54 coated with biologically derived accretions, possibly also with sediment, so analyzing their size and shape

55 and matching them with known objects is a key first step toward identification. This paper focuses on a
56 method to use features on a man-made object to compare it to both historical photographs as well as an
57 exemplar specimen for identification. Photos of the exemplar specimen were adjusted into an
58 orthographic view. The features were then quantitatively compared to the object of interest and also to
59 historical photos of the aircraft taken prior to the crash.

60 In our previous publication on the same subject matter, we detailed our methodology for
61 superimposing CAD models of landing gear on underwater video [10]. In that case study, a man-made
62 rope was visible adjacent to two pieces of purported landing gear. The two CAD model overlays allowed
63 for independent measurements of the diameter of the reference rope, which showed that the rope
64 statistically had the same diameter and that the rope had an appropriate diameter for aircraft tie-down
65 rope. This indicated that both of the objects seen in the video were of the correct scale and general shape
66 of the landing gear on the wrecked aircraft. However, a goodness of fit of the overlays could not be made
67 due to the geometry of the components. In the present analysis, the repeated rivet patterns provide a
68 unique opportunity to allow a goodness of fit calculation to be performed on a new object located at the
69 same site.

70 **1.1. Background**

71 In this case study, we describe using the superimposition of CAD models using underwater video as
72 source data to assess the geometry of objects purported to be from the July 2, 1937 crash site of Amelia
73 Earhart's lost airplane, a Lockheed Electra Model 10E, construction number 1055, off of the island of
74 Nikumaroro in the western Pacific Ocean. This airplane has an overall length of approximately 11.8 m, a
75 wingspan of 16.8 m, and a height of 3.1 m (Figure 1). The outer skin of the aircraft was attached using
76 rivets, and a section of rivets along the window slide rail appeared to match the objects seen in the
77 underwater video.



78

79 **Figure 1:** Amelia Earhart's Lockheed Electra Model 10E aircraft. Scanned from *Lockheed Aircraft since*
80 *1913*, by René Francillon. Photo credit USAF.

81

82 We received the video for analysis retrospectively and we were tasked with extracting as much
83 information as possible from the video footage itself. During an internal review of the video, two objects
84 were identified which resembled a series of rivets. Rivet patterns covering the aircraft were reviewed and
85 the closest resemblance was the rivets located at the window slide rail. Due to the remoteness of the crash
86 site and difficulty involved in safely retrieving the objects, the objective of this study was to assess the
87 geometry of the purported airplane component to determine whether additional investigation of these
88 objects, such as retrieval, is merited.

89

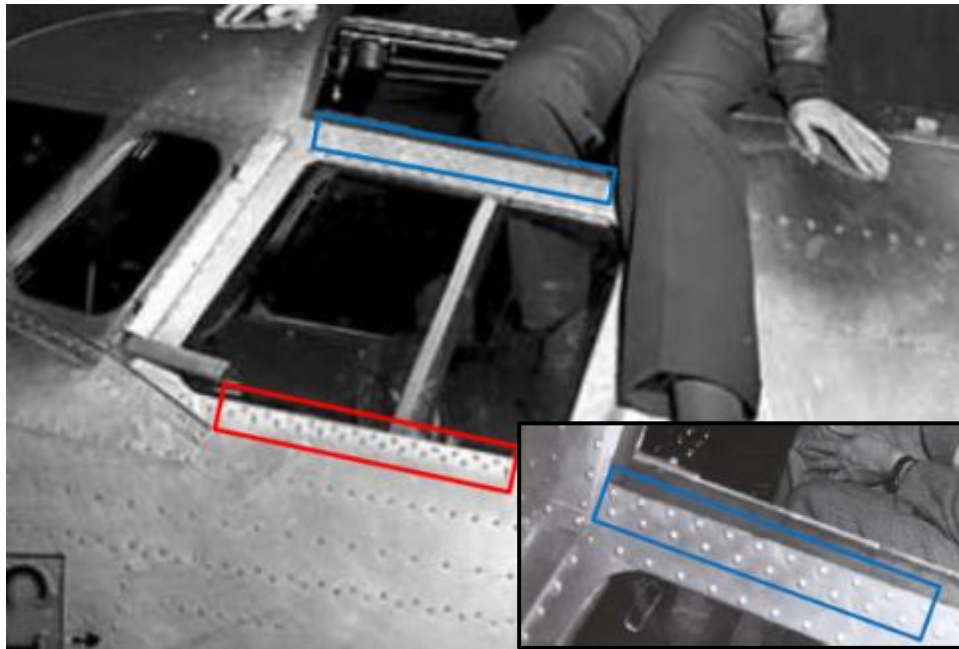
90 **2. Methodology**

91 Using the provided video, we identified two potentially man-made objects, shown in Figure 2. The
92 top object contains a series of repeating, staggered features on a rectangular or cylindrical base. A second
93 object, perpendicular to the first, contains two long, parallel edges. The left side of the second object
94 contains a series of repeating, staggered features, similar to those on the first object. These objects were
95 investigated further because they presented features that bore a resemblance to a rivet pattern seen on the
96 aircraft in Figure 3, and they were located in the suspected crash site.



97

98 **Figure 2:** An object was identified in the suspected underwater crash site.



99

100 **Figure 3:** A photograph illustrating a similar pattern of rivets on the aircraft was taken prior to the crash.

101 We first found historical photos of the aircraft from which the potential piece of wreckage is believed
102 to have originated. Historical photographs of the aircraft were reviewed to identify possible matches to

103 the rivet pattern seen in the purported wreckage. The most visually similar parallel features and rivet
104 patterns were located at the window slide rail (red, Figure 3 and Figure 4) and below the hatch (blue,
105 Figure 3).

106 An aircraft of the same make and model as the one at the potential crash site was used for
107 measurement of the identified rivet pattern, using photographs supplied by the owner of the aircraft. The
108 window slide rail of the intact aircraft contained parallel features, and rivets (Figure 4) that were similar
109 to those seen in the wreckage image (Figure 2) and the historical aircraft (Figure 2).

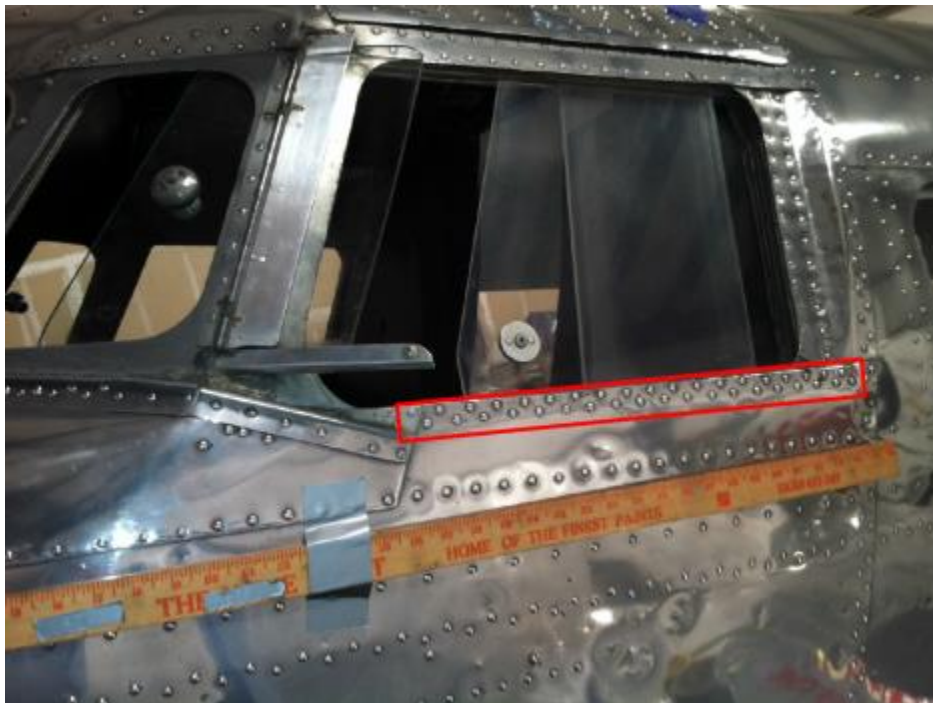


110

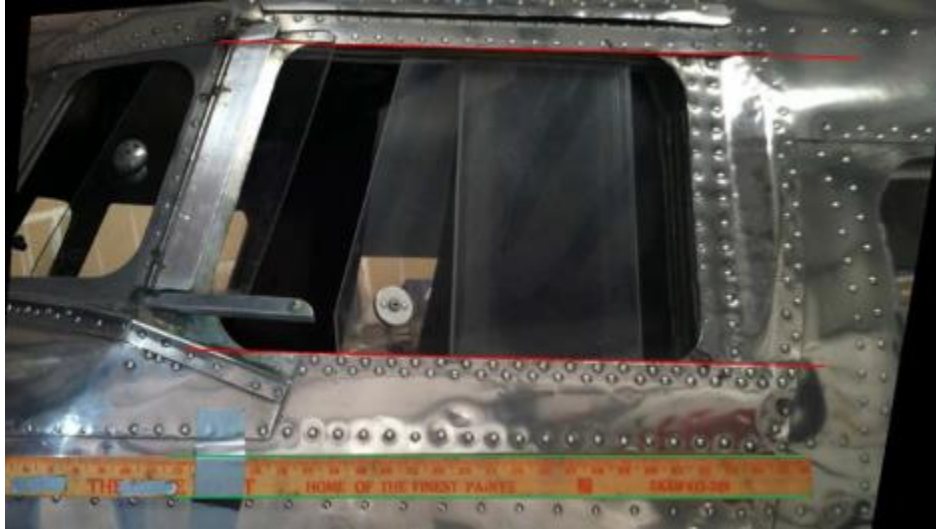
111 **Figure 4:** Parallel rails constrain the side window and allow it to slide.

112 A yard stick was placed in the field of view of each photograph of the intact aircraft (Figure 5). In
113 order to take more accurate measurements from the photograph of the window slide rail, an orthographic

114 transformation of the angled photograph was performed using MATLAB in order to view the window
115 from a perpendicular view (Figure 6). Orthographic projections preserve both distances and angles, and
116 there is no distortion of shape for two-dimensional transformations [11]. The yard stick, having a known
117 length, width, and shape was used as a reference to perform the transformation, with the assumption that
118 the outer face of the window slide rail and yard stick was parallel. The transformed view is orthographic
119 for all features contained in the same plane as the yard stick. The transformed image can be used to
120 measure objects contained in the same geometric plane, such as the rivets on the outside of the slide rail.
121 After the transformation, it is seen that the rectangular geometry and uniform spacing of the yardstick is
122 preserved (Figure 6).



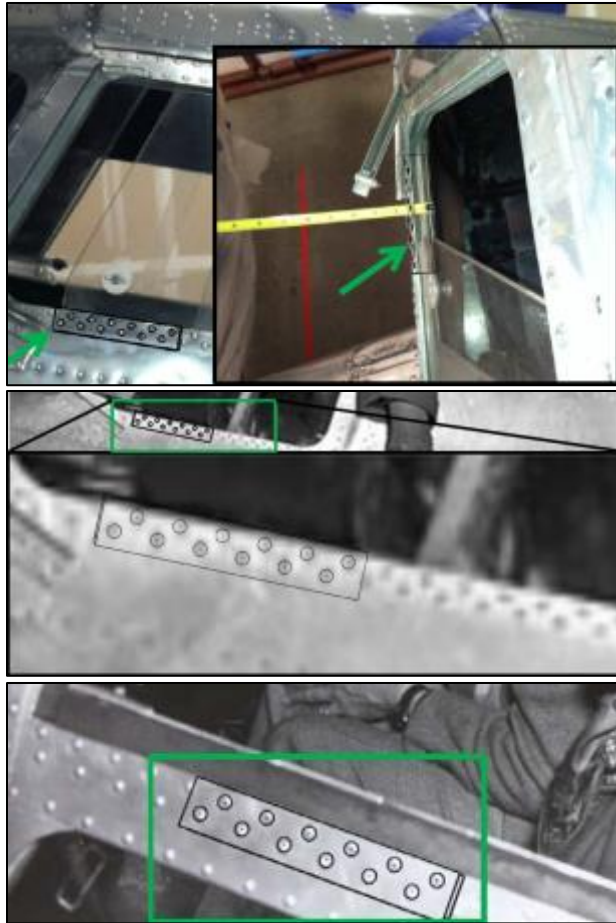
123
124 **Figure 5:** The reference aircraft photograph was not taken perpendicular to the yard stick or rivets.



125

126 **Figure 6:** The photograph of the reference aircraft was transformed to a perpendicular, orthogonal view.

127 A 3D CAD model of the window rail was created using measurements taken from the transformed
128 image (Figure 6) and another photograph of the window slide rail (Figure 4). A rivet diameter of 8 mm
129 was specified. The fits were visually verified with overlays on photos of the intact aircraft and historical
130 photos of the subject historical aircraft (Figure 7).



131

132

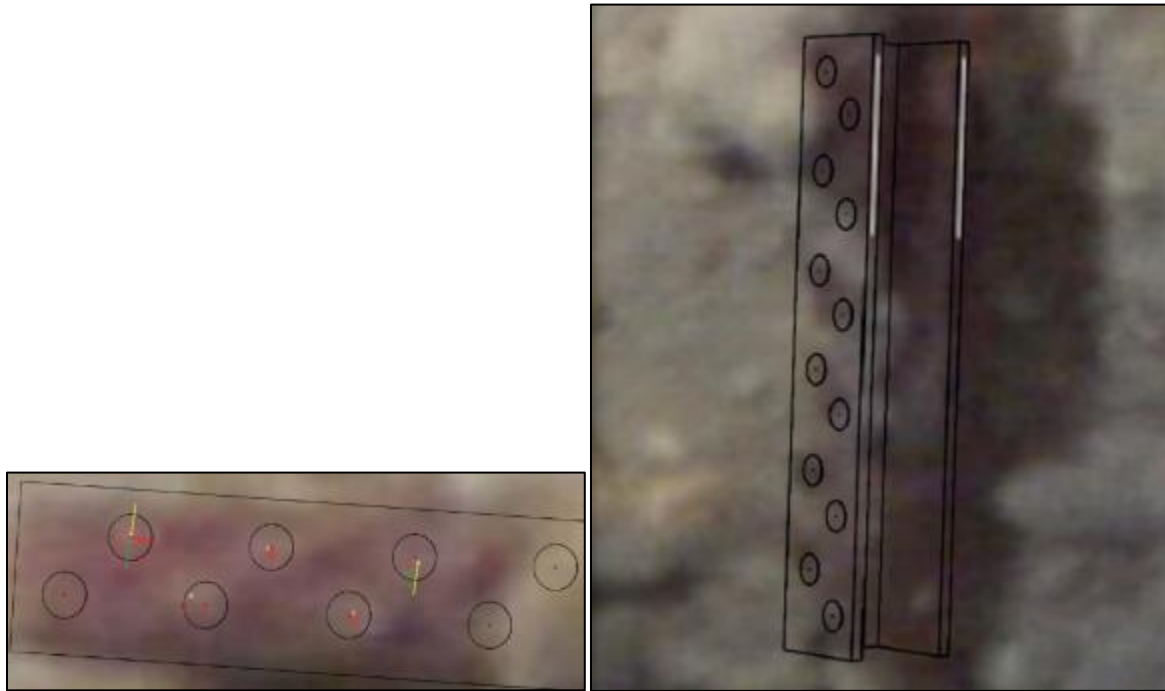
133

134 **Figure 7:** The CAD model was overlaid on the reference aircraft (top) and on historical photos of the
135 crashed aircraft (middle and bottom).

136 Other sections of rivets seen in the historical photographs the plane, such as those seen in front of the
137 roof hatch and behind the side window, were not good fits for the CAD model. However, another section
138 of rivets, located below the roof hatch in the aircraft (bottom, Figure 7), shared the same size and spacing
139 as the series of rivets below the side window.

140 For the underwater objects, the estimated center of the purported rivets on the top object, along with
141 the parallel features on the bottom object, were drawn on a de-interlaced still frame from the video of the
142 wreckage where visually identifiable centers could be ascertained. The CAD model of the purported
143 objects was then overlaid in a perspective view onto the original, still frame, obtaining the best visual fit,
144 similar to what was performed in Figure 7 with the historical photograph overlays. Separately, to reduce
145 observer bias, the centers of the purported rivets were visually identified and marked on the image. The

146 original image with the CAD overlay was then replaced by the marked-up image to measure the level of
147 fit (Figure 8).



148
149 **Figure 8:** The CAD model of the window slide rail was overlaid onto marked-up images from the
150 wreckage video.

151 3. Theory/Calculation

152 In order to provide a quantitative measurement of the misalignment error of individual rivets, the
153 distance between each CAD rivet and the corresponding center of each purported rivet was measured
154 within Solidworks. As a measure of the overall scaling error, a worst-case measurement was taken, which
155 used the farthest-spaced CAD rivets and the farthest-spaced purported rivets as references.

156 By comparing the center of the CAD model rivets to the centers of the purported rivets in the
157 wreckage image, the level of fit can be defined as follows:

158 Center of the staggered shapes perfectly align with the centers of the rivets = Perfect fit

159 Center of the staggered shapes aligns with the edge (radius) of the rivets = Limit of fitting

160 Center of the staggered shapes is outside the radius of the rivets = Not a fit

161 Numerically,

$$162 \quad \text{Fit} = 100\% - 100 * \frac{\sum_{k=1}^n \text{Distance from center point}_k}{\sum_{k=1}^n \text{Radius of rivet}_k}$$

163 With the radius of the rivet used as the reference, the degree of fit can be expressed as a percentage
164 numerically as:

165 Perfect fit = 100%

166 Limit of fitting = 0%

167 Not a fit < 0%

168

169 Therefore, there is a fit if the value is between 0% and 100%, and there is not a fit if the value is
170 negative.

171

172 4. Results

173 When the CAD model is overlaid on the image of the wreckage, the centers of the rivets do not
174 perfectly align. The distance between these centers was measured. The average error, or mean of these
175 distances, was 1.3 mm with an arithmetic standard deviation of 1.1 mm (N=8). The distance between the
176 centers of the corresponding, farthest-spaced CAD model rivets measured 52.6 mm. The distance between
177 the centers of the farthest-spaced purported rivets in the wreckage image measured 53.3 mm. The
178 difference between these measurements gives an overall scaling error of 0.7 mm.

179 Every measured point on the image from the ROV video is located within the radius of the rivets, and
180 using the collected data, there is an 84% fit between the rivets and the centers of the staggered objects
181 seen in the video.

182 Furthermore, using the equation for percentage error, and applied to the worst-case scenario of using
183 the farthest-spaced rivets to measure the error between the image from the ROV video and the CAD
184 model, the error is 1.3%, or conversely, has a fit of 98.7% using this metric:

185
$$\text{Percent Error} =$$

186
$$\frac{\text{Video Image Distance} - \text{CAD model distance}}{\text{CAD model distance}} * 100$$

187 In addition, for the vertically-oriented object, the long edges of the rail aligned with the edges of the
188 vertical object in the rover image to within 3.18 mm, the approximate thickness of the sheet metal,
189 establishing a second correspondence between the CAD model and the objects on the sea floor.
190 Furthermore, there are additional repeating, staggered features toward the bottom of this vertical object,
191 but the vertical object appears nonuniformly bent. Therefore, it was not useful to perform a numerical
192 analysis of this section of the object.

193

194 5. Discussion

195 The approach we used was designed to mitigate any bias or compounded errors, and so provides a
196 powerful way to assess the match between objects at a crash site and known reference objects. Each rivet
197 pattern was measured independently of one another. The CAD models of the rivet patterns from each
198 photograph were also built individually in SolidWorks. The CAD models were visually overlaid onto the
199 ROV image, and an assessment of the goodness of fit was made using the position of the center of rivets.
200 We also calculated a worst case fit from the rivets with the largest discrepancy between the ROV video
201 and CAD model. This gave us an acceptably low percentage error of 1.3%.

202 It is important to keep in mind that a low error simply means that the selected features of the
203 geometry have little difference between the object in the image and the CAD model. An alternative
204 explanation for the origin of the object is that it is naturally made. It was investigated whether this object

205 is a skeletal fragment of a hard coral (order Scleractinia) or a soft coral (subclass Octocorallia, also known
206 as Alcyonaria). These are very diverse groups that are represented by many species in the shallow coral
207 reefs that grow in shallow waters above the study area [12–15]. Some species grow as tubular colonies,
208 either branched or unbranched. They have wood-like or calcareous (limestone) skeletons and, when
209 colonies die their skeletons are frequently broken by storms so that tubular skeletal fragments are likely to
210 be found amongst reef debris fields and be washed into deeper water. Branch fragments vary widely in
211 potential size, and the range of possible sizes spans the estimated size of the unknown object. Skeletal
212 fragments could also plausibly match the unknown object in color, because some Octocorallia can have
213 pink or red colonies whose color would persist for a while after death. Alternatively, the white skeletons
214 of Scleractinians may become pink after death if colonized by crustose coralline algae. Most importantly,
215 colonies have polyps, each of which creates a small bump on the branch, and polyps are sometimes found
216 in alternating rows, like those on the unknown object.

217 Ideally, one or more skeletal fragments of known identity would be compared geometrically to the
218 unknown object using the same method we describe for the window slide rail. We screened shallow-water
219 ROV video from the site and confirm that members of both taxonomic groups (Scleractinia and
220 Octocorallia) with the appropriate branching growth form were present in the area (Figure 9 and Figure
221 10, respectively). Defining specific objects for analysis would, however, require either a return trip to the
222 site to retrieve fragments, or identifying candidates to species from the ROV video, neither of which was
223 possible.



224

225 **Figure 9:** Still image from video recorded in shallow waters near the purported wreckage site illustrating
226 hard coral, order Scleractinia.



227

228 **Figure 10:** Still image from video recorded in shallow waters near the purported wreckage site
229 illustrating soft coral, subclass Octocorallia.

230 In principle, however, it would be best to obtain examples of several plausible reference objects,
231 whether man made or natural, for comparison with an unknown object identified during a search. In our
232 case study, the ROV search was focused on locating a specific aircraft, which provided a rationale for
233 selecting the chosen aircraft model for comparison. In other search contexts, it might be valuable to apply
234 our method to multiple man-made objects (e.g. riveted fittings from multiple known aircraft models) so

235 that the relative goodness of fit of the unknown to a set of plausible reference objects could be judged. In
236 this way, some candidate matches could be excluded, and the search focused by a process of elimination.

237 The method we developed could be applied quite generally and used for other pieces of wreckage in
238 underwater searches. The man-made objects we were searching for have been exposed for nearly a
239 century. Even with the degradations, silt, and natural growth around it we were able to successfully
240 employ this approach to verify that the unknown objects were a close geometric match to the window
241 slide rail on the lost aircraft that was the subject of the search. The same approach will be of most value
242 in other applications where there is some pre-existing documentation of the potential identity of the
243 unknown objects, so that a small set of plausible alternative reference objects can be specified.

244 Extensions of the presented approach might involve using Structure from Motion to form a more
245 complete model of the object to aid in determining the true position of surface features. Better quality
246 video could help alleviate some of the blur and improve the accuracy of points.

247

248 **6. Conclusion**

249 An object in the submarine video was identified as potentially being the window slide rail of a
250 Lockheed Electra Model 10E aircraft. A CAD model of the slide rail was created from measurements
251 taken from a reference aircraft, was overlaid on a still image of the video and goodness of fit
252 measurements were performed.

253 The rivets of the CAD model taken from the reference aircraft's side window slide rail aligned with
254 objects seen in the rover image with an 84% fit.

255 This series of rivets also fit the series of rivets located below the cockpit roof hatch on the historical
256 photographs of the wrecked aircraft. This pattern of rivets did not fit the series of rivets in front of the
257 cockpit roof hatch or behind the side window as seen in historical photographs (Figure 3:). A worst-case
258 measurement comparing the distance between the farthest-spaced rivets had a fit of 98%. The parallel
259 edges in the rover image aligned within the width of the rails of the CAD model.

260 Using the methods outlined in this paper we were able to identify a possible match between part of a
261 lost airplane and an object observed only from underwater video filmed in an area of very limited access.
262 From the video we extracted a still frame of a potential man-made object. The object was inspected and
263 the patterns present on the surface were matched to those found on an historical photograph of the
264 aircraft. The same pattern was independently compared to the patterns on a photograph of an extant
265 exemplar aircraft with a worst-case goodness of fit of 98.7%. Videos of the shallow waters surrounding
266 the purported wreckage were reviewed by a marine biologist to assess the likelihood of a natural origin of
267 the object. Soft and hard corals were identified, but none were identified to have exhibited a similar
268 pattern to the subject object. Based on the available data, it is more likely than not within a reasonable
269 degree of scientific certainty that the object is from a Lockheed Electra Model 10E. The methods
270 described herein provide a valuable method to identify unknown objects by comparing their size and
271 shape to that of known reference.

272

273 **7. References**

- 274 [1] G. Telem, S. Filin, Photogrammetric modeling of underwater environments, ISPRS J.
275 Photogramm. Remote Sens. 65 (2010) 433–444.
- 276 [2] G. Telem, S. Filin, Photogrammetric modeling of the relative orientation in underwater
277 environments, ISPRS J. Photogramm. Remote Sens. 86 (2013) 150–156.
278 doi:10.1016/j.isprsjprs.2013.10.001.
- 279 [3] O. Barkai, Y. Kahanov, The Tantura F Shipwreck, Israel, Int. J. Naut. Archaeol. 36 (2007) 21–31.
280 doi:10.1111/j.1095-9270.2006.00114.x.
- 281 [4] M. Canciani, P. Gambogi, F.-G. Romano, G. Cannata, P. Drap, low cost digital photogrammetry
282 for underwater archaeological Site survey and artifact isertion. The case study of the dolia Wreck
283 in secche della meloria-livorno-italia, ISPRS Work. Vis. Tec. Digit. Archit. Archaeol. Arch.
284 (2003) ?
- 285 [5] C. Wöhler, P. d’Angelo, L. Krüger, A. Kuhl, H.-M. Groß, Monocular 3D scene reconstruction at
286 absolute scale, ISPRS J. Photogramm. Remote Sens. 64 (2009) 529–540.
287 doi:10.1016/j.isprsjprs.2009.03.004.
- 288 [6] O. Faugeras, Three-dimensional Computer Vision: A Geometric Viewpoint, MIT Press, 1993.
- 289 [7] J. Battle, E. Mouaddib, J. Salvi, Recent progress in coded structured light as a technique to solve
290 the correspondence problem, Pattern Recognit. 31 (1998) 963–982. doi:10.1016/S0031-
291 3203(97)00074-5.
- 292 [8] Y.Y. Schechner, N. Kiryati, Depth from Defocus vs. Stereo: How Different Really Are They?, Int.
293 J. Comput. Vis. 39 (2000) 141–162. doi:10.1023/A:1008175127327.
- 294 [9] P. D’Angelo, C. Wöhler, Image-based 3D surface reconstruction by combination of photometric,
295 geometric, and real-aperture methods, ISPRS J. Photogramm. Remote Sens. 63 (2008) 297–321.
296 doi:10.1016/j.isprsjprs.2007.09.005.

- 297 [10] J.M. Vincelli, F. Calakli, M.A. Stone, G.E. Forrester, T. Mellon, J.D. Jarrell, Characterizing a
298 Debris Field Using Digital Mosaicking and CAD Model Superimposition from Underwater Video,
299 Photogramm. Eng. Remote Sens. 82 (2016) 223–232. doi:10.14358/PERS.82.3.223.
- 300 [11] M. Shah, K. Rakesh, Video Registration, Springer Science & Business Media, 2003.
- 301 [12] J.E. Maragos, A.M. Friedlander, S. Godwin, C. Musburger, R. Tsuda, E. Flint, O. Pantos, P.
302 Ayotte, E. Sala, S. Sandin, S. McTee, D. Siciliano, D. Obura, US coral reefs in the Line and
303 Phoenix Islands, central Pacific Ocean: status, threats and significance, Coral Reefs USA. (2008)
304 643–654. doi:10.1007/978-1-4020-6847-8_16.
- 305 [13] D. Obura, Coral reef structure and zonation of the Phoenix Islands, Atoll Res. Bull. (2011) 63–82.
306 doi:10.5479/si.00775630.589.63.
- 307 [14] D. Obura, S. Mangubhai, Coral mortality associated with thermal fluctuations in the Phoenix
308 Islands, 2002-2005, Coral Reefs. 30 (2011) 607–619. doi:10.1007/s00338-011-0741-7.
- 309 [15] S.A. Sandin, J.E. Smith, E.E. DeMartini, E.A. Dinsdale, S.D. Donner, A.M. Friedlander, T.
310 Konotchick, M. Malay, J.E. Maragos, D. Obura, O. Pantos, G. Paulay, M. Richie, F. Rohwer, R.E.
311 Schroeder, S. Walsh, J.B.C. Jackson, N. Knowlton, E. Sala, Baselines and degradation of coral
312 reefs in the Northern Line Islands, PLoS One. 3 (2008). doi:10.1371/journal.pone.0001548.
- 313